# A quantative comparison of two restoration methods as applied to confocal microscopy

*Geert M.P. van Kempen[1], Hans T.M. van der Voort[2], Lucas J. van Vliet[1]*

[1] Pattern Recognition Group, Delft University of Technology, Lorentzweg 1, 2628 CJ Delft, The Netherlands
[2] Scientific Volume Imaging B.V., J. Geradtsweg 181, 1222 PS Hilversum, The Netherlands

## 1. Introduction

The main contribution of the confocal microscope to microscopy is that it provides a practical method to obtain microscopic volume images. Although a confocal microscope is a true volume imager, its imaging properties give rise to a blurring phenomenon similar to that of a conventional microscope, but with a reduced range. The resulting distortions hamper subsequent quantitative analysis. Therefore, operations that invert the distortions of the microscope may improve these analyses. In previous work [1], the iterative constrained Tikhonov-Miller (ICTM) inversion was used to restore diffraction-induced distortions. Quantitative texture measurements, based on the grey value distance transform (GDT) [2], showed that the results improved when applied to images after restoration.

The use of the ICTM restoration method was motivated by the linear system model of the imaging properties of a confocal microscope. In this model, the image is a convolution of the object with the microscopes point spread function and distorted by additive noise.

However in images with a low signal-to-noise ratio (SNR), this additive noise model is a poor description of the actual photon-limited image recording. Under these circumstances, the noise characteristics are best described by a Poisson process, which motivates the use of restoration methods optimized for Poisson noise distorted images.

We have compared the ICTM inversion with the expectation-maximization algorithm for computing the maximum likelihood estimator (EM-MLE) for the intensity of a Poisson process

## 2. Image restoration methods

The incoherent nature of the emitted fluorescence light allows us to model the image formation of the confocal fluorescence microscope (CFM) as a convolution of the object $f$ with the confocal point spread function $h$ (CPSF) of the microscope, The image $g$ formed by an ideal noise free CFM can thus be written as

$$g(y) = \int_X h(y-x) f(x) dx \tag{1}$$

with $x$ being a coordinate in the object space $X$, and $y$ in the image space $Y$. Due to the photon nature of light and its effect on $f$, $g$ is distorted by noise. Noise, caused by photon-counting, by the readout of the detector, and by the analog-to-digital conversion, disturbs the image. We model this noise distortion here in a general way

$$m(y) = N\big(g(y)\big) \tag{2}$$

with $m(y)$ being the recorded image and $N()$ the noise distortion function.

G.M.P. van Kempen, H.T.M. van der Voort, and L.J. van Vliet, A quantitative comparison of two restoration methods as applied to confocal microscopy, Proc. ASCI'96, 2nd Annual Conf. of the Advanced School for Computing and Imaging (Lommel, Belgium, June 5-7), ASCI, Delft, 1996, 196-201.

Restoration methods are based on finding an approximate solution $\hat{f}$, given *g* and *h*, from a set of feasible solutions according to certain criteria. These criteria depend on the type of noise, imposed regularization, and constraints set on the solutions found by the restoration algorithm. Although both the EM-MLE algorithm as the ICTM inversion are in principle based on maximum likelihood estimation, they differ significantly due to the different modeling of noise distortion on the image and imposed constraints and regularization.
The EM-MLE computes the maximum likelihood estimate of the intensity of a Poisson process [9]. The ICTM inversion is a constrained, regularized mean-square-error restoration method for finding a non-negative solution for images distorted by additive noise.

***The EM-MLE Algorithm***

A confocal microscope acquires an image of an object by scanning the object in three dimensions. At each point of the image, the emitted fluorescence light from the object is focused on a photo multiplier tube (PMT). Under low light-level conditions, the PMT detector behaves essentially as a photon counter. This conversion of fluorescence intensity to a discrete number of detected photons is described statistically as a Poisson process. The log likelihood function of equation (2), for *N()* being a Poisson process, is given by [3]

$$L\left(\hat{f}\right) = -\int_Y \hat{g}(y)dy + \int_Y \ln\left[\hat{g}(y)\right] m(y)dy \tag{3}$$

with $\hat{g}$ the convolution of the $\hat{f}$ and *h*. The maximum likelihood solution for $\hat{f}$ can be found using the EM algorithm, as described by Dempster, Laird and Rubin[4]. The EM-MLE solution for Eq. (3) is [9]:

$$\hat{f}_{k+1}(x) = \hat{f}_k(x) \int_Y \left[ \frac{h(x-y)}{\int_X h(y-x)\hat{f}_k(x)dx} \right] m(y)dy \tag{4}$$

The EM-MLE algorithm insures non-negative solution, when non-negative initial guess $\hat{f}_1$ is used. Snyder et al.[5] have shown that maximizing the mean of the log likelihood of Eq. (3) is equal to minimizing Csiszár's I-Divergence [19],

$$I\left(f, \hat{f}\right) = L(f) - E\left[L\left(\hat{f}\right)\right] = \int_Y \left( \ln\left[\frac{g(y)}{\hat{g}(y)}\right] g(y) - g(y) + \hat{g}(y) \right) dy \tag{5}$$

with *E*[ ] the expectation operator.

***The Iterative Constrained Tikhonov-Miller inversion***

The ICTM inversion is based on the assumption that the noise distortion function *N()* can be modeled as an additive noise function[6]. For images with a relatively high SNR, the additive noise model can be motivated by the Central Limit theorem: Under these circumstances, the distribution of a Poisson process can be approximated with a Gaussian distribution.
The Tikhonov-Miller (TM) inversion combines two selection criteria for finding $\hat{f}$ in one quadratic functional

$$\Phi\left(\hat{f}\right) = \left\| g - h \otimes \hat{f} \right\|^2 + \left(\frac{\varepsilon}{E}\right)^2 \left\| \hat{f} \right\|^2 \tag{6}$$

with $\varepsilon$ the noise power and $E$ the power of the object. The TM functional consists of a mean-square-error (MSE) criterion and an energy bound. This bound suppresses solutions of $\hat{f}$ that oscillating wildly due to spectral components outside the bandwidth of $h$. Direct minimization of Eq. (6) yields the well-known TM solution,

$$\hat{F} = \frac{H^* G}{\|H\|^2 + \eta} \tag{1}$$

with $\eta = (\varepsilon/E)^2$ and capitals the Fourier transform of the corresponding function. Although this solution requires modest computational efforts, it is a linear solution, thus not capable of restoring missing frequency components. Furthermore, the solution may contain negative values, which is a major drawback, since the intensity of light intensity is by definition positive.

A solution to these disadvantages is to solve Eq. (6) with an iterative procedure, the ICTM method. It constrains the solution $\hat{f}$ to be non-negative, by clipping each successive estimate. We used the method of conjugate gradients to iteratively find the TM inversion [6]. The so-called conjugate direction is given by

$$p_k = r_k + \frac{\|r_k\|}{\|r_{k-1}\|} p_{k-1} \tag{2}$$

with $r_k$ denoting the steepest descent direction,

$$r_k = -\frac{1}{2} \nabla_f \Phi\left(\hat{f}\right) = \left(\|h\| + \eta\right) \hat{f}_k + h^* \otimes g \tag{3}$$

A new conjugate gradient estimate is now found as

$$\hat{f}_{k+1} = \hat{f}_k + \beta p_k \tag{4}$$

In absence of a non-linear constraint, the step size ß can be calculated analytically. However, in the presence of such a constraint, the optimal ß must be searched for iteratively.

**3. Experiments and Results**

In a first experiment, we compared the results of EM-MLE and ICTM algorithms on simulated spheres convolved with a CPSF and distorted with Poisson noise. The spheres were generated using an analytical description of their Fourier transform [7]. The Fourier transform of the sphere is multiplied by the Fourier transform of the CPSF to ensure bandlimitation. We computed the CPSF from a theoretical model based on electromagnetic diffraction theory [1]. Generated in this way, the spheres are free from aliasing effects which arise from sampling non-bandlimited analytical objects.

The restoration results were compared using the MSE and I-Divergence[8] because the investigated restoration methods minimize these distances measures.

Figure 1 shows the I-Divergence and MSE performance of the EM-MLE and ICTM methods on the restoration of spheres as a function of the SNR (figure 2). The I-Divergence and the MSE performance of EM-MLE is in most cases an order of magnitude better than ICTM. Only

for high SNR, the MSE performance of ICTM approaches EM-MLE. The SNR (defined as $E/\varepsilon$) ranges from 1.0 to 256.0.

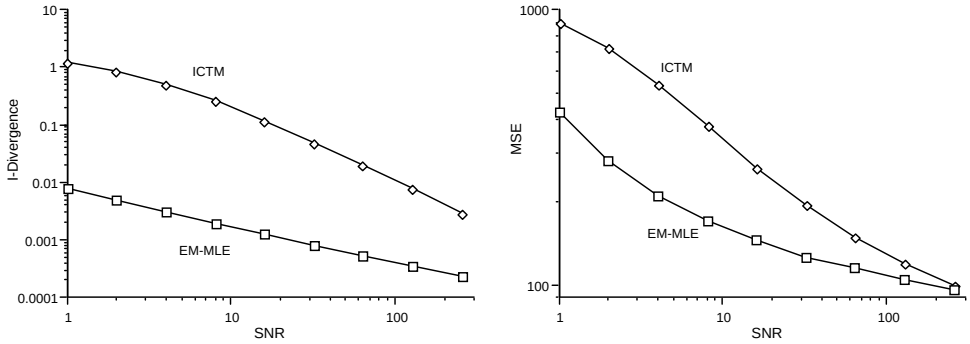


Figure 1 The I-Divergence and MSE of the EM-MLE and ICTM restoration of spheres.

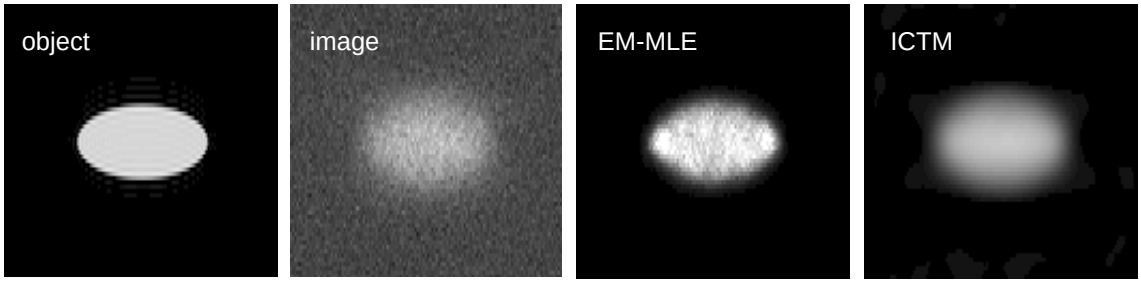


Figure 2 Restoration of spheres. the object, the confocal image with a SNR of 16.0 and the results of the EM-MLE and ICTM algorithms.

In a second experiment, we investigated the influence of the restoration methods on the CPSF measurement technique as has been used by Van der Voort and Strasters [1]. We used their approach, and compare the ICTM results with EM-MLE (figure 3 and 4).

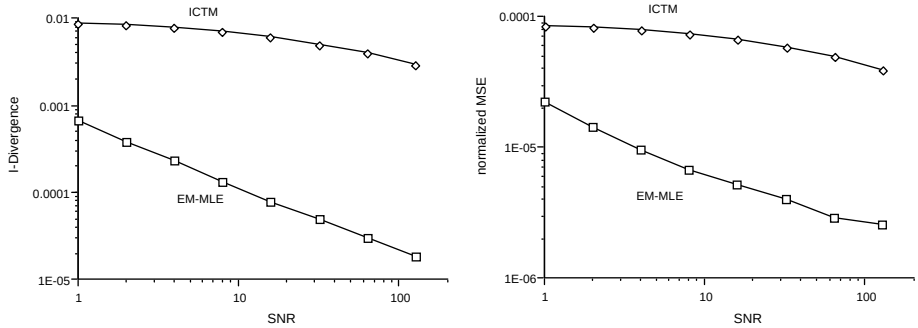


Figure 3 The I-Divergence and MSE of the EM-MLE and ICTM result of the CPSF restoration. The MSE is normalized by dividing it by the squared maximum intensity of the CPSF.

In a third experiment, the influence is investigated of EM-MLE and ICTM on a quantitative texture analysis. The restoration methods were used prior to a quantitative texture measure based on the GDT [2]. The experiment was performed as function of the angle of the object with respect to the focal plane This angle varies the distance between the objects in the *z*-direction, in which most of the blurring occurs.

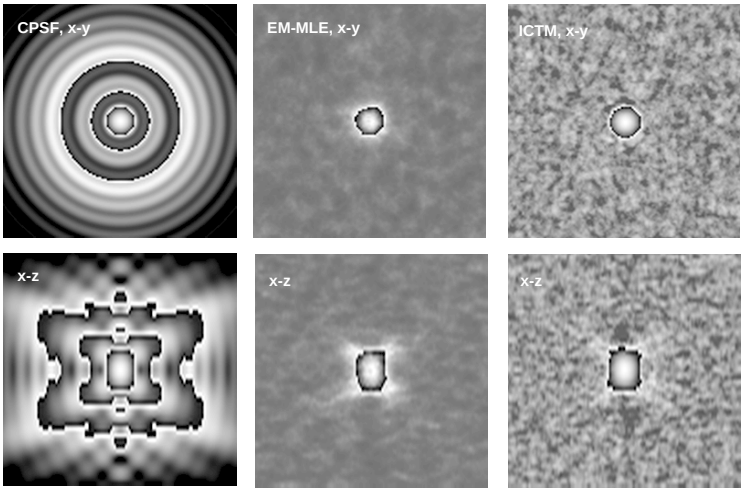


Figure 4 Restoration of the CPSF. The left pictures show the center *x-y* and *x-z* planes of the theoretical CPSF. The middle two pictures show EM-MLE result, with the ICTM result on the right. Each transition from black to white represent an intensity reduction of a factor of ten.

The GDT sum values of the confocal image of the generated cylinders, as well as the values of the EM-MLE and ICTM results are shown in Fig. 5. This figure shows a considerable reduction of the GDT sum value for ICTM. The reduction of the EM-MLE reconstructed images is an order of magnitude better than the ICTM results. However, the % error of the EM-MLE values are negative in most cases, indicating a smaller GDT value for the EM-MLE result than for the object.

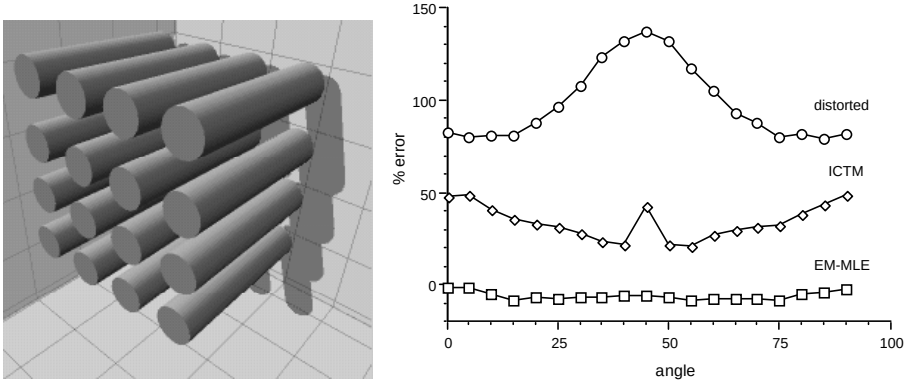


Figure 5 **Left:** Schematic model of the multiple cylindrical objects as used in the third experiment. **Right:** Error in the GDT texture measure before and after restoration with EM-MLE and ICTM. *Horizontal axis:* object's rotation angle with respect to the focal plane. *Vertical axis:* percentage of the relative error between the GDT values derived from the (restored) image and of the object.

For our simulations, we have selected microscope parameters corresponding to typical working conditions: a numerical aperture of 1.3, a refractive index of 1.515, an excitation wave length of 479 nm, and a pinhole size of 282 nm. The images were generated with a sampling density of twice the Nyquist frequency. An important motivation for this choice is given by the multiplicative iterative updating of the EM-MLE algorithm (Eq. (4)). The spatial multiplication of $\hat{f}$ results in a convolution of $\hat{F}$ in the Fourier domain, giving rise to potential aliasing effects. By sampling at above the Nyquist frequency, these aliasing effects are reduced.

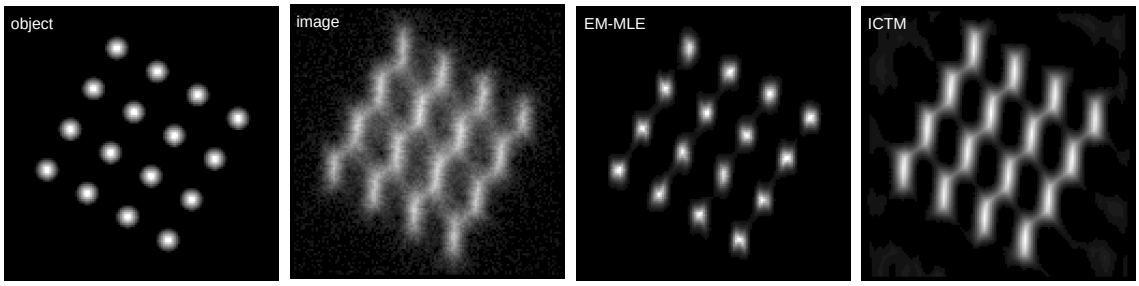

Figure 6 The GDT of the images used in the third experiment

## 4. Conclusions

We have compared the performance of the EM-MLE and ICTM restoration algorithms applied to confocal images. Both methods greatly reduce diffraction-induced distortions of confocal images. From our experiments it is clear that for our test objects the EM-MLE algorithm performs much better than ICTM. It produces better results under all the conditions we tested, and with respect to all three performance measures (I-Divergence, MSE, GDT) we used. Only for high SNR conditions, the MSE performance of ICTM approaches the EM-MLE results. The poor ICTM performance shows that its functional is not well suited for images distorted with Poisson noise.

We did not find artifacts such as ringing in the results of either algorithm. The restoration results on the cylindrical objects show however that the EM-MLE algorithm has a tendency to reconstruct an image which is sharper and smaller than the original object (Fig. 6). This aspect of EM-MLE should be investigated thoroughly. Greander's method of Sieves [3] seems a promising method for regularizing the EM-MLE algorithm.

## Acknowledgement

This work was partially supported by The Netherlands Organization for Scientific Research (NWO) and the ASCI PostDoc program.

## References

1. Van der Voort HTM, Strasters KC*: Restoration of confocal images for quantitative image analysis*. J of Microscopy 178 (2): 165-181, 1995.
2. K.C. Strasters, A.W.M. Smeulders, and H.T.M. van der Voort, *3-D texture characterized by accessibility measurements, based on the grey weighted distance transform*, BioImaging, vol. 2, no. 1, 1994, 1-21.
3. Snyder DL, Miller MI*: Random Point Processes in Time and Space*, 2nd Edition, Springer-Verlag, New York, 1991.
4. Dempster AP, Laird NM, Rubin DB*: Maximum Likelihood from Incomplete Data via the EM Algorithm*. J of the Royal Statistical Society B 39: 1-37, 1977.
5. Snyder DL, Schutz TJ, O'Sullivan JA: *Deblurring subject to Nonegative Constraints*. IEEE Trans on Signal Processing 40, pp 1143-1150, 1992.
6. Lagendijk RL: *Iterative identification and restoration of images*, PhD thesis, Delft University of Technology, 1990.
7. Van Vliet LJ: Grey-scale *Measurements in multi-dimensional digitized Images*, PhD Thesis, Delft University Press, Delft, The Netherlands, 1993.
8. Csiszar I: *Why Least Squares and maximum entropy? An axiomatic approach to inference for linear inverse problems.* The Annals of Statistics 19 (4): 2032-2066, 1991.